Automatic Bottom-Following for Underwater Robotic Vehicles

Aras Adhami-Mirhosseini [a], Mohammad J. Yazdanpanah [a], A. Pedro Aguiar [b]

[a] *Control and Intelligent Processing Center of Excellence, University of Tehran, P.O. Box 14395/515 Tehran, Iran.*

[b] *Faculty of Engineering, University of Porto (FEUP), Rua Dr. Roberto Frias, 4200-465 Porto, Portugal.*

Abstract

In this note we propose a solution for the automatic bottom-following problem for a low cost autonomous underwater vehicle. We consider the case that the seabed profile is not known in advance, and we show that it is possible to solve the bottom-following using only one echo sounder and without the need to measure the vertical velocity component (heave velocity). To this effect, we propose an output feedback controller that is obtained by first re-formulating the bottom-following into a trajectory tracking problem, then constructing a reference signal generator (the exo-system) using Fourier series theory, and finally solving the control design problem in the framework of nonlinear output regulation theory. An interesting feature of this approach is that the combination of the Fourier series with output regulation problem allows to bypass the need to compute explicitly the Fourier coefficients. To obtain an approximate solution of the resulting regulator equations we resort to pseudo-spectral methods. Stability analysis that takes explicitly into account the effects of the inner-loop autopilots, disturbances, and measurement noise is presented. Simulation results with real seabed data show the effectiveness of the proposed controller.

Key words: Bottom-following; AUVs; Nonlinear Output Regulation.

1 Introduction

The bottom-following or seabed tracking problem has been identified as one core task in an increasing number of scientific (and military) applications that require autonomous underwater vehicles (AUV) to execute traverses at a constant altitude from the sea bottom.

One of the first works reported in the literature on bottom-following using underwater vehicles can be traced in (Bennett *et al.*, 1995) where proportional integrator type controllers are proposed. In (Caccia *et al.*, 2003), a Lyapunov based controller for a Remotely Operated Vehicle (ROV) is developed that uses the estimated altitude and seabed slope from the measurements given by two echo sounders. Another method proposed in (Silvestre *et al.*, 2009) for bottom-following takes into account the terrain characteristics ahead of the vehicle that are also provided by two echo sounders. The main idea amounts to formulate the problem as a discrete time path following control task, where a conveniently defined state error in the space model of the plant is augmented with bathymetric preview data.

This paper is concerned with the case that the seabed profile is not known in advance and with the additional restriction that the proposed bottom-following solution is to be applied to small low cost AUVs that have limited navigation sensors. In particular, we consider the case that there is only a single beam acoustic altimeter sensor, and furthermore, it does not carry on-board a device (e.g., a DVL) that provides the linear heave (vertical) velocity w. It is important to stress that the above mentioned limitations pose considerable challenges for control design and to the best of authors knowledge there are no bottom-following solutions that address such important practical case.

In this note, we design an output feedback bottom-following control algorithm that exploits the output regulation framework and pseudo-spectral methods to approximate the solutions of the regulator equations. To this effect, the main idea is to first re-formulate the bottom-following as a trajectory tracking problem, then construct an exo-system by resorting to Fourier series

⋆ This paper was not presented at any IFAC meeting. Corresponding author A. P. Aguiar. Tel. +351 22 041 3282

Email addresses: a.adhami@ece.ut.ac.ir (Aras Adhami-Mirhosseini), yazdan@ut.ac.ir (Mohammad J. Yazdanpanah), pedro.aguiar@fe.up.pt (A. Pedro Aguiar).

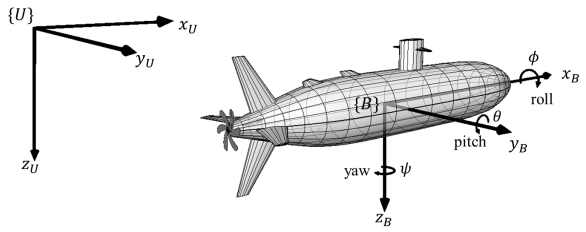

Fig. 1. Coordinate frames, positions and orientations of an AUV

to approximate the seabed profiles, and finally solve the control design problem in the framework of nonlinear output regulation theory. An interesting feature of this approach is that the combination of the Fourier series with output regulation problem allows to bypass the need to compute explicitly the Fourier coefficients, and further, the resulting dynamic controller embodies naturally an observer of the seabed profile. We also consider the practical situation that there exist inner-loop tracking controllers for the linear surge velocity u and pitch angular rate q and take their dynamics explicitly into account in the stability analysis and control design. In particular, we show that the tracking error converges to a small neighborhood of zero, whose size depends on the size of the external disturbances and measurement noise, and also on the fact of not having perfect inner-loop autopilots. With ideal autopilots (infinite bandwidth) and in the absence of disturbances and noise, the error converges to zero.

The paper is organized as follows: Section 2 describes the nonlinear model for the vertical plane dynamics of an AUV and formulates precisely the addressed bottom-following problem. Section 3 states the output feedback controller design procedure, and in Section 4 the stability analysis is discussed. In Section 5, the performance of the proposed control algorithm is evaluated using computer simulations and real seabed data. Section 6 contains concluding remarks. Part of this work was presented in preliminary form in (Adhami-Mirhosseini *et al.*, 2011).

2 Control problem formulation

This section describes the AUV equations of motion used for control design and formulates the bottom-following problem. Fig. 1 illustrates the AUV coordinate frames, position and orientation variables. In general, the motion of an AUV can be described using six degrees of freedom (DOF) differential equations of motion, which can be highly nonlinear and coupled, see e.g., (Fossen, 1994). In practice, the procedure adopted to simplify the controller design, is to split the equations into two non-interacting models for the vertical and horizontal planes, (Jalving, 1994). For the bottom-following case and for control design, we are concerned with the vertical plane and we follow the model simplification strategy. Later, it will be shown that this strategy is indeed adequate because the closed-loop system is locally stable as long as the neglected coupling terms are locally bounded. Further, simulation results with the complete six degrees of freedom model shows that the impact on the closed-loop performance is almost negligible. In the vertical plane, the kinematic equations take the form

$$\dot{x} = u\cos\theta + w\sin\theta \tag{1a}$$
$$\dot{z} = -u\sin\theta + w\cos\theta \tag{1b}$$
$$\dot{\theta} = q \tag{1c}$$

where u, w and q are the linear and angular velocities of the vehicle, respectively, in surge (x_B), heave (z_B) and pitch (θ) direction of the body-fixed coordinates $\{B\}$. The Cartesian coordinates of the vehicle's center of mass is denoted by x and z, and θ is the pitch angle. Collecting in the vector $\tau_e = (\tau_{e_u}, \tau_{e_w}, \tau_{e_q})$ the effects of the environmental disturbances, neglected coupling terms, and unmodeled dynamics, the simplified equations of motion for surge, heave, and pitch rate when there is no actuated force in Z_B direction (that is, the vehicle is underactuated) yield

$$m_u\dot{u} + m_w wq + d_u(u)u = \tau_u + \tau_{e_u} \tag{2a}$$
$$m_w\dot{w} - m_u uq + d_w(w)w = 0 + \tau_{e_w} \tag{2b}$$
$$m_q\dot{q} + m_{uw}uw + d_q(q)q - z_B B\sin\theta = \tau_q + \tau_{e_q} \tag{2c}$$

where $m_u = m - X_{\dot{u}}$, $m_w = m - Z_{\dot{w}}$, $m_q = I_y - M_{\dot{q}}$ and $m_{uw} = m_u - m_w$ are mass and hydrodynamic added mass terms, $d_u(u) = -X_u - X_{u|u|}|u|$, $d_w(w) = -Z_w - Z_{w|w|}|w|$ and $d_q(q) = -M_q - M_{q|q|}|q|$ are hydrodynamic damping effects, and B denotes the buoyancy. The values of these scalar parameters are listed in the simulation section for a particular AUV. In the equations, and for clarity of presentation, it is assumed that the AUV is neutrally buoyant and that the center of buoyancy can be expressed as $(x_B, y_B, z_B) = (0, 0, z_B)$, where z_B is the metacentric height. The symbols τ_u and τ_q denote the actuated force in surge direction and torque around the y-axis of the vehicle, respectively.
We consider the practical situation that there exist inner-loop controllers in charge of tracking reference signals in u and q, and that these autopilots controllers can be even characterized by an n-order nonlinear dynamics as long as locally the origin of the related linearized unforced dynamics are asymptotically stable. For simplicity, in the paper we will assume that they are locally characterized by first order stable dynamics.

The bottom-following problem can be stated as follow: *Consider the AUV vertical model (1) and (2) together with measurements on the depth z and altitude h from the seabed. Derive output feedback control laws for the surge reference velocity u_r and pitch rate reference velocity q_r*

to drive the vehicle to move along an X_B direction with a desired horizontal velocity V_d at a specified constant height h_d from the seabed.

3 Controller design

In this section we derive the output feedback control laws to solve the bottom-following problem. In what follows we will neglect the term τ_e and the dynamics of the inner-loop feedback laws. They will be explicitly taken into account in the stability analysis section.

Step 1: Converting the bottom-following into a trajectory tracking problem

Let $z_s(x)$ be the (unknown) seabed profile that we would like the vehicle to track and let T_x be a given predefined length. Using Fourier series (Steffens, 2006), we can approximate z_s by a finite combination of N sinusoidal functions with frequencies $\Omega_i = \frac{2\pi}{T_x} i$, amplitude A_i and phase φ_i, i.e.,

$$\hat{z}_s(x) = A_0 + \sum_{i=1}^{N} A_i \sin(\Omega_i x + \varphi_i) \tag{3}$$

To represent (3) as a function of time, we first compute the surge velocity reference $u_r(t)$ for the speed controller such that the horizontal velocity of the vehicle is regulated to the desired value V_d. In this case, from (1) it follows that

$$u_r = \frac{V_d - w \sin\theta}{\cos\theta} \tag{4}$$

where we have assumed that the pitch angle of the vehicle is not close to the singular points $(2k \pm 1)\pi/2$, which in practice for this type of marine vehicles is a reasonable assumption. Later, u_r in (4) will be redefined to address the fact of not requiring measurements of the heave velocity w.

From (4) we can now conclude that when $u = u_r$ we have $\dot{x} = V_d$ and therefore $x(t) = V_d(t - t_0) + x(t_0)$. Without loss of generality set $t_0 = 0$ and $x(0) = 0$. By this relation between time and horizontal position, the seabed profile (3) can be rewritten as a time dependent signal

$$\hat{z}_s(t) = A_0 + \sum_{i=1}^{N} A_i \sin(\Omega_i V_d t + \varphi_i) \tag{5}$$

This reference signal can be produced by the following autonomous neutrally stable system recalled exo-system

$$\begin{aligned} \dot{\xi} &= S\xi \\ S &= V_d \,\mathrm{Diag}\left(0, \begin{bmatrix} 0, & \Omega_1 \\ -\Omega_1, & 0 \end{bmatrix}, \ddots, \begin{bmatrix} 0, & \Omega_N \\ -\Omega_N, & 0 \end{bmatrix}\right) \end{aligned} \tag{6}$$

where $\xi \in \mathbb{R}^{2N+1}$ is the state vector. The output y_s of the exo-system is defined as $y_s = [1\ 1\ 0\ 1\ 0 \ldots 1\ 0]\xi$. By setting the proper initial conditions to the exo-system, the reference signal (5) is equal to the output of the exo-system, i.e. $\hat{z}_s(t) = y_s(t)$ for all $t \geq 0$. Later, it will be clear that the resulting controller will include a subsystem, which can be viewed as an observer of the seabed profile that receives continuously the measurement signals of the depth z and altitude h and outputs an estimate of the seabed z_s. In fact, this observer uses (6) and takes the form $\dot{\hat{\xi}} = S\hat{\xi} - L(z + h - F\hat{\xi})$, $\hat{z}_s = F\hat{\xi}$ with appropriate matrices L and F.

The AUV equations with $u = u_r$ is reduced to

$$\dot{x}_p = f_p(x_p, q) \tag{7}$$

where $x_p = [z, w, \theta]^T$ and

$$f_p = \begin{bmatrix} -V_d \tan\theta + \frac{w}{\cos\theta} \\ \frac{Z_w}{m_w} w + \frac{Z_{w|w|}}{m_w} w\,|w| + \frac{m_u}{m_w}\left(\frac{V_d}{\cos\theta} - w\tan\theta\right) q \\ q \end{bmatrix}$$

At this point, we have converted the bottom-following into an equivalent trajectory tracking problem with the additional feature of being in the framework of the nonlinear output regulation (NOR) problem with plant model (7), exo-system (6) and error $e = y_s - z - h_d$. To simplify the notation in design procedure, we replace $z + h_d$ by z. Thus, hereafter the output to be regulated is changed to $e = y_s - z$.

Step 2: Output regulator design

Using the nonlinear output regulation methodology, see e.g., (Isidori, 1995; Marconi and Praly, 2008; Huang, 2004; Pavlov *et al.*, 2006), we propose a dynamic controller of the form

$$\begin{aligned} \dot{\eta} &= \sigma(\eta, y_m) \\ q_r &= k(\eta, y_m) \end{aligned} \tag{8}$$

where y_m satisfies the output equation

$$\begin{aligned} y_m &= \begin{bmatrix} z \\ z_s \end{bmatrix} = C_m x_p + F_m \xi, \qquad C_m = \begin{bmatrix} 1 & 0 & 0 \\ 0 & 0 & 0 \end{bmatrix}, \\ F_m &= \begin{bmatrix} & 0 & \\ 1 & 1 & 0 \cdots 1 \quad 0 \end{bmatrix}. \end{aligned} \tag{9}$$

Note that in (8), y_m will be a signal provided by the set of sensors that measure the depth z and the altitude h (where $z_s = z + h$). Later we will consider and analyze the real situation of these measurements being corrupted

by noise. Returning to the design procedure, we first derive a state feedback controller $q_r = \alpha_q(\xi) + K(x_p - \pi(\xi))$, where $\alpha_q(\xi)$ and $\pi(\xi) = [\pi_z(\xi), \pi_w(\xi), \pi_\theta(\xi)]^T$, with $\alpha_q(0) = 0$ and $\pi(0) = 0$, are mappings resulting from the solution of the regulator equations

$$\begin{aligned}
\tfrac{\partial \pi_z}{\partial \xi} S\xi &= -V_d \tan \pi_\theta + \tfrac{\pi_w}{\cos \pi_\theta} \\
\tfrac{\partial \pi_w}{\partial \xi} S\xi &= \tfrac{Z_w}{m_w}\pi_w + \tfrac{Z_{w|w|}}{m_w}\pi_w |\pi_w| \\
&\quad + \tfrac{m_u}{m_w}\left(\tfrac{V_d}{\cos \pi_\theta} - \pi_w \tan \pi_\theta\right)\alpha_q \qquad (10) \\
\tfrac{\partial \pi_\theta}{\partial \xi} S\xi &= \alpha_q \\
0 &= [1\ 1\ 0\ 1\ 0 \ldots 1\ 0]\xi - \pi_z
\end{aligned}$$

The matrix gain K is computed such that the state-space matrix of the closed-loop linearized system of the reduced plant model (7) at the origin $A_K = A_p + B_p K$ is Hurwitz. In the above, $A_p = \frac{\partial f_p}{\partial x_p}\Big|_{(0,0)}$ and $B_p = \frac{\partial f_p}{\partial q}\Big|_{(0,0)}$ are the state and input matrix of the linearized reduced model (7).

Now, the dynamic controller takes the form

$$\dot{\eta}_1 = f_p(\eta_1, q_r) - L_1\left(y_m - C_m \eta_1\right) \qquad (11a)$$
$$\dot{\eta}_2 = S\eta_2 - L_2\left(y_m - F_m \eta_2\right) \qquad (11b)$$
$$q_r = \alpha_q(\eta_2) + K\left(\eta_1 - \pi(\eta_2)\right) \qquad (11c)$$

where $\eta_1 \in \mathbb{R}^3$ and $\eta_2 \in \mathbb{R}^{2N+1}$ are controller states that estimate x_p and ξ, respectively. The matrices L_1 and L_2 are computed such that

$$A_L = \begin{bmatrix} A_p & 0 \\ 0 & S \end{bmatrix} + \begin{bmatrix} L_1 \\ L_2 \end{bmatrix} \begin{bmatrix} C_m & F_m \end{bmatrix} \qquad (12)$$

is Hurwitz. Note that the reference signal u_r for the surge velocity in (4) can now be modified to use the estimated states $\eta_1 = [\eta_z, \eta_w, \eta_\theta]^T$ as follows

$$u_r = \frac{V_d - \eta_w \sin \eta_\theta}{\cos \eta_\theta} \qquad (13)$$

Step 3: Obtaining an approximated solution of the regulator equations

A typical problem that arises in the NOR framework is the fact that in general there is no closed form solution of the regulator equations. The computation of an approximation solution is an alternative way to overcome this difficulty. For that effect, one of the oldest methods is to use truncated Taylor series expansion, which is an easy method in computation and complexity. We did not follow that approach since for our case, the Taylor fails in accuracy because it is too local (not good when $\xi \in \mathbb{R}^{2N+1}$ is not so close to the origin) and also the regulator equation (10) is not smooth. To solve the problem of convergency and accuracy in distant point, we propose to use a pseudo-spectral method because it offers high accuracy with fast convergence in approximation order and reasonable computational complexity. The main idea is to compute the solution to the regulator equation (10) at some collocation points $\xi^{[i]} \in \mathcal{I}$ for $i = 1, \ldots, m_a$ in a rectangular subspace $\mathcal{I} \subset \mathbb{R}^{2N+1}$, and approximate $\pi(\xi)$ and $\alpha_q(\xi)$ by

$$\begin{aligned}
\pi(\xi) &\approx \textstyle\sum_{i=1}^{m_a} \pi(\xi^{[i]}) l_i(\xi) \\
\alpha_q(\xi) &\approx \textstyle\sum_{i=1}^{m_a} \alpha_q(\xi^{[i]}) l_i(\xi)
\end{aligned} \qquad (14)$$

where $l_i(.), i = 1, \ldots, m_a$ are Lagrange bases polynomials with respect to the selected collocation points, which attains value 1 at one of the collocation points and vanishes in the others. Lagrange bases are not unique, a simple choice is

$$l_i(\xi) = \prod_{\substack{k=1 \\ k \neq i}}^{m_a} \prod_{j=1}^{2N+1} \frac{\xi_j - \xi_j^{[k]}}{\xi_j^{[i]} - \xi_j^{[k]}}, \qquad i = 1, \ldots, m_a \qquad (15)$$

Note that by substituting the approximated mapping (14) into the regulator equations (10) and isolating the obtained equation at the i^{th} collocation point, we have

$$\begin{aligned}
\textstyle\sum_{i=1}^{m_a} \frac{\partial l_i}{\partial \xi}\Big|_{\xi^{[i]}} S\xi^{[i]} \pi(\xi^{[i]}) &= f_p\left(\pi(\xi^{[i]}), \alpha_q(\xi^{[i]})\right) \\
0 &= [1\ 1\ 0\ 1\ 0 \ldots 1\ 0]\xi^{[i]} - \pi_z(\xi^{[i]})
\end{aligned} \qquad (16)$$

Thus, writing these algebraic equations at all collocation points, and denoting $\bar{\Pi}^T = \big[\pi(\xi^{[1]})^T, \cdots, \pi(\xi^{[m_a]})^T, \alpha_q(\xi^{[1]}), \cdots, \alpha_q(\xi^{[m_a]})\big]$, we obtain a system of nonlinear algebraic equations compactly written as

$$D\bar{\Pi} = F_p(\bar{\Pi}) \qquad (17)$$

where $D \in \mathbb{R}^{4m_a \times 4m_a}$ is called the derivative matrix formed by properly ordering the known coefficients of the left hand side of (16), and $F_p \in \mathbb{R}^{4m_a}$ is a nonlinear vector function constructed from the right hand side of (16). The algebraic equation (17) can be solved using a simple numerical method. The number of collocation points m_a is related to the approximation order that is set and depends on the required accuracy. For further details of the pseudo-spectral method see (Funaro, 1991) and (Fornberg, 1996).

4 Stability analysis

We now analyze the stability and performance of the proposed output feedback controller in closed-loop with sinusoidal seabed profiles, assuming exact solution of

$$A_{11} = \begin{bmatrix} A_K & B_p \begin{bmatrix} K & , & D \end{bmatrix} \\ 0 & & A_L \end{bmatrix} \qquad A_{12} = \begin{bmatrix} 0 & , & \begin{bmatrix} B_p \\ \begin{bmatrix} -B_p \\ 0 \end{bmatrix} \end{bmatrix} \end{bmatrix}$$

$$A_{21} = \begin{bmatrix} b_y^T L_1^T H_u & & b_y^T L_1^T H_u \begin{bmatrix} I_3 & 0 \end{bmatrix} \\ -KA_K & - \begin{bmatrix} K & D \end{bmatrix} A_L + \begin{bmatrix} -KB_pK & b_y^T L_2^T H_q - KB_pD \end{bmatrix} \end{bmatrix} \qquad A_{2\xi} = \begin{bmatrix} b_y^T L_1^T H_u \Pi \\ -KA_K\Pi - DS - KB_pD + b_y^T L_2^T H_q \end{bmatrix}$$

$$A_{22} = \begin{bmatrix} -\lambda_u & 0 \\ 0 & -\lambda_q \end{bmatrix} \qquad B_1 = \begin{bmatrix} 0 & 0 & 0 \\ -L_1 & 0 & 0 \\ -L_2 & 0 & 0 \end{bmatrix} \qquad B_2 = \begin{bmatrix} 0 & 1 & 0 \\ KL_1 + DL_2 & 0 & 1 \end{bmatrix} \tag{20}$$

the regulator equations, but with non negligible inner-loop dynamics, measurement noise and the presence of bounded disturbances. To address explicitly the inclusion of the inner loop dynamics, thus lifting the unrealistic assumption that the actual surge u and pitch rate q equals the desired surge u_r and q_r, respectively, we define the mismatch errors as $\tilde{u} = u - u_r$ and $\tilde{q} = q - q_r$, and consider that the autopilots characteristics in closed-loop can be locally described (for simplicity) by a first order dynamics. More precisely, we assume that

$$\dot{\tilde{u}} = -\lambda_u \tilde{u} - \dot{u}_r + b_u \tag{18a}$$
$$\dot{\tilde{q}} = -\lambda_q \tilde{q} - \dot{q}_r + b_q \tag{18b}$$

where b_u and b_q are bounded unknown disturbances due to (but not only) the external disturbances τ_e defined in (2), and $\lambda_u, \lambda_q > 0$ are the convergence rates (bandwidths) of the autopilots. It is important to stress that (18a) (and similarly to (18b)) matches locally what is perceived in practice: if the reference u_r is constant, then the autopilot will make the vehicle converge to a neighborhood (with a small error) of the desired reference; whereas for time-varying references the autopilot will have more difficulty (depending on the bandwidth) to keep the tracking error small. Notice also that we have assumed first order dynamics, but the next results can be extended for n-order nonlinear dynamics as long as the origin of the related linearized dynamics are asymptotically stable. In that case, (18a) would be replaced by $\dot{x}_u = A_u x_u + B_u \dot{u}_r$, and $\tilde{u} = C_u x_u + b_u$, with A_u Hurwitz.

Theorem 1 *Consider the AUV equations of motion in the vertical plane (1) and* (2) *together with the inner-loop tracking dynamics* (18)*, the seabed profile of the type (3) and the dynamic output feedback controller* (11)*, where π and α_q are the solution to the regulator equations (10) in some neighborhood $\mathcal{W} \subset \mathbb{R}^{2N+1}$ of the origin. Consider also that the measurement signal y_m in* (11) *is corrupted with additive bounded noise b_y, that is, replace y_m by $y_m + b_y$. Then, there exists a value $\lambda^\star > 0$ such that if $\lambda_u, \lambda_q > \lambda^\star$ it follows that for sufficiently small initial conditions, the closed-loop system has bounded states, and the vehicle altitude $h = z_s - z$ converges to a small neighborhood of the desired constant distance h_d from the seabed. Furthermore, in the absence of disturbances and noise, and with ideal autopilots (infinite bandwidth), the altitude $h(t)$ satisfies $\lim_{t\to\infty} h(t) = h_d$.*

PROOF.

Define the error vectors $\tilde{x}_1 = [x_p - \pi(\xi), \eta_1 - x_p, \eta_2 - \xi]^T$ and $\tilde{x}_2 = [\tilde{u}, \tilde{q}]^T$. Consider the bounded measurement noise b_y and the bounded disturbances in (18) gather in the perturbation vector $w_b = [b_y, b_u, b_q]^T$. After straightforward computations it can be concluded that the closed-loop dynamics can be written in the form

$$\dot{\tilde{x}}_1 = A_{11}\tilde{x}_1 + A_{12}\tilde{x}_2 + B_1 w_b + \phi_1(\tilde{x}_1, \tilde{x}_2, \xi) \tag{19a}$$
$$\dot{\tilde{x}}_2 = A_{21}\tilde{x}_1 + A_{22}\tilde{x}_2 + A_{2\xi}\xi + B_2 w_b + \phi_2(\tilde{x}_1, \tilde{x}_2, \xi) \tag{19b}$$
$$\dot{\xi} = S\xi \tag{19c}$$

where $\phi_i, i = 1, 2$ vanish at the origin with their first order derivatives. The state and input matrices in (19) are defined in (20) with $B_p = \frac{\partial f_p}{\partial q}\Big|_{(0,0)}$, $\Pi = \frac{\partial \pi(\eta_2)}{\partial \eta_2}\Big|_{(0)}$, $D = \frac{\partial \alpha(\eta_2)}{\partial \eta_2}\Big|_{(0)} - K\Pi$. The Hessian matrices H_u and H_q are given by $H_u = \frac{\partial}{\partial \eta_1}\left(\frac{\partial u_r}{\partial \eta_1}\right)^T\Big|_{(0)}$ and $H_q = \frac{\partial}{\partial \eta_2}\left(\frac{\partial q_r}{\partial \eta_2}\right)^T\Big|_{(0)}$.

At this point we could use the center manifold theory combined with the theory of singular perturbations to conclude Theorem 1. We decided not to follow this path because we would like to obtain performance bounds of the steady state solution. To this end, we use the results (Lemma 2) described in the Appendix.

Assume first the case of absence of noise and disturbances, that is, $w_b = 0$. In this case, using a first order approximation, the interconnected subsystems (19a) and (19b) can be recognized as the one in Fig. 6, where $\xi(t)$ is a forced bounded input. Since the upper triangular matrix A_{11} is Hurwitz from the fact that A_K and A_L are designed to be Hurwitz and A_{22} is a diagonalizable Hurwitz matrix with $\underline{\lambda}(A_{22}) = \min(\lambda_u, \lambda_q)$, by Lemma 2 it follows that there exists a positive constant λ^* such that for any $\lambda_u, \lambda_q > \lambda^*$ the equilibrium point $\tilde{x} = (\tilde{x}_1, \tilde{x}_2) = (0, 0)$ is locally stable. Moreover, the time evolution of $\tilde{x}(t)$ satisfies the following inequality with a decreasing function $\rho : \mathbb{R}^+ \to \mathbb{R}^+$, $\rho(0) = 0$,

$$\lim_{t\to\infty} \sup |\tilde{x}(t)| \leq \rho\left(\underline{\lambda}(A_{22})\right)\|\xi\|_\infty$$

In this case, the seabed tracking problem is achieved practically, i.e.,

$$\lim_{t\to\infty} \sup |h(t) - h_d(t)| \leq \rho\left(\min(\lambda_u, \lambda_q)\right)\|\xi\|_\infty$$

From the application of Lemma 2, it can be also concluded that for infinite bandwidth inner-loop controllers, i.e., $\lambda_u, \lambda_q \to \infty$, the seabed altitude tracking error converges to zero.

Now, consider the closed-loop system in the presence of noise and disturbances. The first two subsystems of the linearized error dynamic (19), can be seen as a linear system forced by a bounded exo-signal ξ and bounded disturbances w_b as

$$\dot{\tilde{x}} = A\tilde{x} + B_\xi \xi + B_b w_b \tag{21}$$

where

$$A = \begin{bmatrix} A_{11} & A_{12} \\ A_{21} & A_{22} \end{bmatrix} \quad B_\xi = \begin{bmatrix} 0 \\ A_{2\xi} \end{bmatrix} \quad B_b = \begin{bmatrix} B_1 \\ B_2 \end{bmatrix}$$

It has been shown above that for any $\lambda_u, \lambda_q > \lambda^*$, the matrix A is Hurwitz. Thus, the response of the linear stable system (21) is bounded and satisfies the following inequality

$$\lim_{t\to\infty} \sup |\tilde{x}(t)| \leq \frac{\|B_\xi\|}{\underline{\lambda}(A)}\|\xi\|_\infty + \frac{\|B_b\|}{\underline{\lambda}(A)}\|w_b\|_\infty,$$

which implies that if the closed-loop trajectories start sufficiently close to the origin $(x_p, \eta, \xi) = (0, 0, 0)$, then they remain bounded and the vehicle converges to the desired distance from the seabed with a small error that depends on the bounds of the exo-signal and the disturbances. Note also that as $\lambda_u, \lambda_q \to \infty$, the $\lim_{t\to\infty} \sup |\tilde{x}(t)|$ will be independent of ξ.

Remark: From a practical point of view (important for the tuning of the control parameters), it can be implicitly concluded from Theorem 1 that if the gains K and L of the output regulator are fixed a-priori, then it follows that it is possible to compute a critical value λ^* that corresponds to the point that for sure if the convergence rate of the autopilots are faster, then the closed-loop system is locally stable.

Table 1
AUV parameters

Parameter description	Symbol	Value
Vehicle mass (kg)	m	30
Added masses (kg)	$(X_{\dot{u}},\, Z_{\dot{w}})$	$(-2.2, -4.0)$
Damping (kg/s,kg/m)	$(Z_w, Z_{w\|w\|})$	$(-3, -12.4)$

Table 2
Constant parameters in the simulations

Parameter description	Symbol	Value
Horizontal velocity (m/s)	V_d	0.5
Desired distance (m)	h_d	5
Linear vel. u_r limit (m/s)	-	1
Angular vel. q_r limit (rad/s)	-	0.5
Fourier app. order	N	1
Fourier app. horizon (m)	T_x	100
Controller gain	K	[22.4, 87.3, –55.2]
Observer gain	L_1	$\begin{bmatrix} -4.0 & -2.6 & 3.2 \\ 0 & 0 & 0 \end{bmatrix}^T$
Observer gain	L_2	$\begin{bmatrix} 0 & 0 & 0 \\ -0.4 & -1.4 & -1 \end{bmatrix}^T$

5 Simulation results

To show the effectiveness of the output regulator with measurement feedback, we performed several computer simulations using the complete 6DOF of an AUV model, which contains the nonlinear coupling terms and possible disturbances. To this end, besides the inner-loop autopilots, an heading autopilot was also implemented to address the horizontal plane (states r and ψ) of the AUV. Table 1 shows the values of the nominal parameters used for the proposed bottom-following control design and Table 2 contains the controller parameters and simulation conditions fixed for all simulations.

The control design procedure and its implementation is briefly summarized in Algorithm 1, where a backward Euler method was used for discretization. To make the simulations closer to the practical situation, the vehicle model is discretized by a step size of $0.001\,s$, but the control inputs are computed each $0.01\,s$, and the distance from the seabed is measured each $0.1\,s$. Also, we have included saturations on the desired linear and angular velocities u_r and q_r, respectively.

The first set of simulations is concerned with the tracking

Algorithm 1 Bottom-following procedure

Off-line

Input: Fourier approximation specifications: N and T_x.
Numerical solution specifications: m_a and $\mathcal{I}$.
Vertical model AUV nominal parameters.

Output: Approximate regulator mappings π and α_q.
Controller gains K, L_1, L_2.

1. Construct the matrix S defined in (6).
2. Compute the gains K, L_1, L_2 using for example a linear-quadratic regulator (LQR) method so that A_K and A_L introduced in (Step 2, Section 3) are Hurwitz.
3. Determine the approximation mappings π and α_q, according to (Step 3, Section 3) and save the results in a lookup table.

On-line

Input: Desired horizontal velocity V_d and distance h_d.
Regulator mappings π and α_q (lookup table)
Controller gains K, L_1, L_2

Output: Control signals u_r and q_r.

1. Refresh the measurements: seabed level every 0.01 seconds and the vehicle altitude every 0.1 seconds.
2. Compute the desired velocities q_r and u_r from (11) and (13).
3. Send the computed values of q_r and u_r to the inner-loop autopilots. Go back to 1.

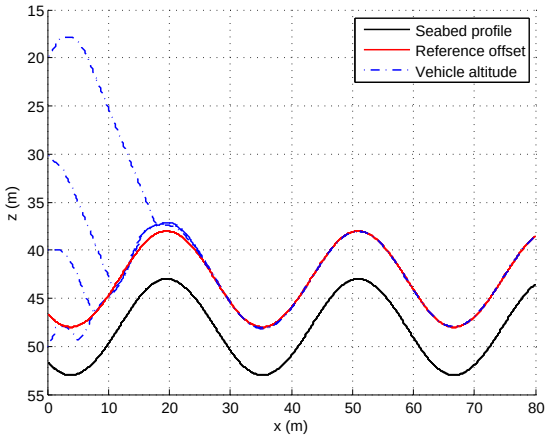

Fig. 2. Trajectories described by the vehicle with output feedback output regulator for a sinusoid seabed profile.

of the sinusoidal seabed $z_s = 48 + 5\sin(0.2x + \frac{\pi}{4})$ with a desired vertical distance $h_d = 5\,m$. Fig. 2 shows the vehicle trajectories starting from four different initial conditions. It can be seen that the proposed controller exhibits good performance even with initial conditions far from the steady state.

A second set of simulations was carried out using a real seabed profile of a volcanic seabed in the Atlantic ocean near Azores. The data was collected in a 1 km^2 area with a horizontal grid resolution of 1 m spacing. Fig. 3 shows a part of the seabed profile and its Fourier first and second order approximations, which can also be obtained from

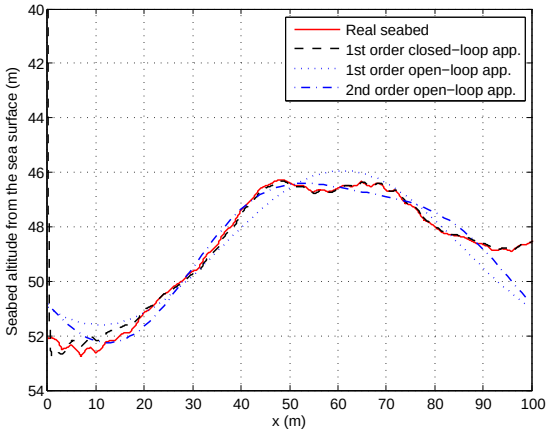

Fig. 3. Fourier approximations of the real seabed profile by the open-loop and closed-loop exo-system

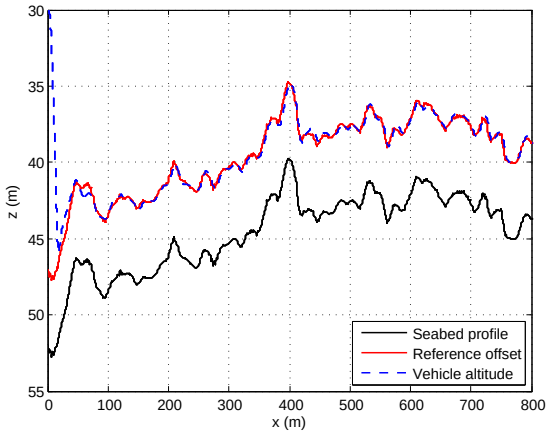

Fig. 4. Trajectory described by the vehicle with output feedback output regulator for a real seabed profile.

the output signal of the (open-loop) exo-system (6) with $N = 1$ and $N = 2$, respectively, and with appropriated initial conditions. For comparison, Fig. 3 also shows the output of the observer described in (11b) that includes the exo-system in closed-loop with initial conditions far from the corrected ones, and with only one harmonic ($N = 1$) of frequency $\Omega_1 = 2\pi/T_x$, $T_x = 100m$. Clearly, the closed-loop approximation is significantly better and furthermore it could be concluded that at least for this type of seabeds, one harmonic is more than enough.

Fig. 4 displays the vehicle trajectory and Fig. 5 shows the time evolution of the tracking error $e = z_s - z - h$, the control inputs and the pitch angle for $t \in [600, 1000]$. The initial conditions of the vehicle for the vertical states were set to $x(0) = 0$, $z(0) = 30$, $w(0) = 0$, $\theta(0) = 0$, and for the controller, $\eta_1(0) = [0, 0, 0]^T$ and $\eta_2(0) = [0, 0, 30]^T$. It is worth noting that the vehicle follows the bottom profile (that is not known a priori) with a fairly small error.

To evaluate the benefits of the output regulator, a com-

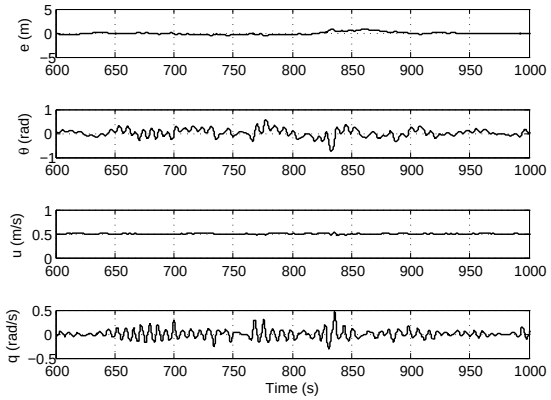

Fig. 5. Time evolution of relevant closed-loop signals with output feedback output regulator for a real seabed profile.

Table 3
Comparison of the proposed and the simpler controllers

Method	Index	Sinusoidal	Real
Output regulation	$\|e_{ss}\|_2$	0.14	0.77
	$\|e_{ss}\|_\infty$	0.08	0.75
Simpler controller	$\|e_{ss}\|_2$	4.88	1.06
	$\|e_{ss}\|_\infty$	1.88	1.11

parison is made with a simpler bottom following controller that is similar to the proposed one, but without the exo-system component. More precisely, equation (11) is substituted by

$$\dot{\eta}_1 = f_p(\eta_1, q_r) - L_1 (z - \eta_z)$$
$$q_r = K \left(\eta_1 - [z_s - h_d, 0, 0]^T\right)$$

where $\eta_1 = [\eta_z, \eta_\theta, \eta_w]^T$, and L_1 is the same observer gain matrix as used for the proposed output regulator. To compare both controllers, we introduce the steady-state tracking error defined as $e_{ss}(t) = z_s(t) - h_d - z(t)$, $t \in [t_{ss}, t_f]$, where t_{ss} is large enough time to guarantee that the transient time is passed and t_f is the final simulation time. The following two quantitative indexes are defined: $\|e_{ss}\|_2^2 = \int_{t_{ss}}^{t_f} e_{ss}^2(t)dt$ and $\|e_{ss}\|_\infty = \sup_{t\in[t_{ss},t_f]} |e_{ss}(t)|$. Table 3 contains the tracking error indexes obtained for the proposed and for the simpler controllers in face of the sinusoidal and the real seabed profiles. From Table 3 it can be concluded that the influence in performance can be significant if the seabed is not flat. In that case, the presence of the exo-system/observer plays a key role.

To investigate the robustness of the proposed controller against model parameter uncertainty, a set of Monte-Carlo simulations runs were carried out. In this case, all the vehicle parameters were randomly perturbed up to $\pm 20\%$ of their nominal values. Table 4 shows the statistical quantities of the tracking indexes after 100 simulations. The results verify that the closed-loop system is not so sensitive to the parameters.

Table 4
Robustness study results against parameters uncertainty

Method	Index	Mean	Var.	Min	Max
Output	$\|e_{ss}\|_2$	0.84	0.03	0.65	1.17
regulation	$\|e_{ss}\|_\infty$	0.87	0.02	0.69	1.17
Simpler	$\|e_{ss}\|_2$	1.08	0.06	0.69	1.55
controller	$\|e_{ss}\|_\infty$	1.10	0.08	0.59	1.57

6 Concluding Remarks

This paper addressed the design of a seabed tracking controller for a low cost AUV. Using the tools of nonlinear output regulation theory combined with Fourier series expansion and pseudo-spectral methods, we have proposed a nonlinear dynamic controller that solves the bottom-following problem without requiring to know in advance the seabed profile and using only one single echo sounder to measure the altitude from the seabed. Stability and zero tracking error of the closed-loop system taking into account the effects of the inner-loop autopilots, disturbances, and measurement noise were analyzed. The performance evaluated through computer simulations indicates that the proposed controller is a good candidate to be implemented in practice.

Appendix

In this Appendix we provide explicit bounds for the trajectories of the interconnected system represented in Fig. 6.

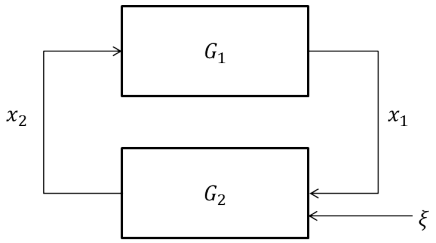

Fig. 6. Interconnected system.

We make use of the following notation: $|\cdot|$ stands for the Euclidean norm of a vector, the infinity norm of a signal $x(t)$ is defined as $\|x(t)\|_\infty = \sup_{t\geq 0}|x(t)|$, and $\|A\|$ (resp. $\|G\|$) is the corresponding induced norm of the matrix (resp. system). For any diagonalizable Hurwitz matrix A, it is not difficult to show

$$\int_0^{+\infty} \|e^{At}\|dt \leq \frac{1}{\underline{\lambda}(A)} \tag{22}$$

where $\underline{\lambda}(A) = \min_i |\lambda_i(A)|$.

Lemma 2 *Consider the interconnected system represented in Fig. 6 of the form*

$$G_1: \quad \dot{x}_1 = A_{11}x_1 + A_{12}x_2, \qquad x_1 \in \mathbb{R}^{n_1} \tag{23a}$$
$$G_2: \quad \dot{x}_2 = A_{22}x_2 + A_{21}x_1 + B\xi, \quad x_2 \in \mathbb{R}^{n_2},\ \xi \in \mathbb{R}^m \tag{23b}$$

where A_{11}, A_{22} are Hurwitz matrices and A_{22} is diagonalizable. There exists a $\lambda^* > 0$ such that if $\underline{\lambda}(A_{22}) > \lambda^*$ the origin $x = 0$ of the overall system is stable and for any bounded input $\xi(t)$ the trajectories $x_1(t)$ and $x_2(t)$ satisfy

$$\begin{aligned} \lim_{t\to\infty} |x_1(t)| &\leq \tfrac{\lambda^*\|B\|}{(\underline{\lambda}(A_{22})-\lambda^*)\|A_{21}\|}\ \|\xi(t)\|_\infty \\ \lim_{t\to\infty} |x_2(t)| &\leq \tfrac{\|B\|}{\underline{\lambda}(A_{22})-\lambda^*}\ \|\xi(t)\|_\infty \end{aligned} \tag{24}$$

Moreover, if $\underline{\lambda}(A_{22}) \to \infty$, then $x(t)$ converges to zero as $t \to \infty$.

PROOF. Since systems G_1 and G_2 are linear, the states responses $x_i(t) = x_i(t; x(0), \xi(t))$, $i = 1, 2$ satisfy

$$x_i(t) = x_i(t; x(0), 0) + x_i(t; 0, \xi(t)), \quad i = 1, 2 \tag{25}$$

First, consider the unforced system, i.e., $\xi(t) = 0$. From the small-gain theorem (Zames, 1966), the interconnected system is stable if $\|G_1\|\|G_2\| < 1$. By the definition of the induced norms of the first (resp. second) subsystem with x_2 (resp. x_1) as input and x_1 (resp. x_2) as output, the stability condition is derived as

$$\|A_{12}\|\|A_{21}\| \int_0^\infty \|e^{A_{11}t}\|dt \int_0^\infty \|e^{A_{22}t}\|dt < 1$$

Considering the inequality (22) for Hurwitz diagonalizable matrix A_{22}, the above stability sufficient condition can be represented as $\underline{\lambda}(A_{22}) > \lambda^*$, where

$$\lambda^* = \|A_{12}\|\|A_{21}\| \int_0^\infty \|e^{A_{11}t}\|dt \leq \frac{\|A_{12}\|\|A_{21}\|}{\underline{\lambda}(A_{11})} \tag{26}$$

Thus, in that case, it follows that the unforced system responses converge to zero, i.e.,

$$\lim_{t\to\infty} x_i(t; x(0), 0) = 0, \quad i = 1, 2 \tag{27}$$

Now, consider the zero-state response of the interconnected system forced by a bounded input $\xi(t)$. The stable linear subsystems' responses satisfy the following inequalities for every $t \geq 0$

$$\begin{aligned} |x_1(t;0,\xi)| &\leq \|A_{12}\| \textstyle\int_0^t \|e^{A_{11}t}\|dt\ \|x_2(t;0,\xi)\|_\infty \\ |x_2(t;0,\xi)| &\leq \|A_{21}\| \textstyle\int_0^t \|e^{A_{22}t}\|dt\ \|x_1(t;0,\xi)\|_\infty \\ &\quad + \|B\| \textstyle\int_0^t \|e^{A_{22}t}\|dt\ \|\xi(t)\|_\infty \end{aligned} \tag{28}$$

Taking the supremum over $t \geq 0$ from inequalities (28) leads to

$$\begin{aligned} \|x_1(t;0,\xi)\|_\infty &\leq \tfrac{\lambda^*}{\|A_{21}\|}\ \|x_2(t;0,\xi)\|_\infty \\ \|x_2(t;0,\xi)\|_\infty &\leq \tfrac{\|A_{21}\|}{\underline{\lambda}(A_{22})}\|x_1(t;0,\xi)\|_\infty + \tfrac{\|B\|}{\underline{\lambda}(A_{22})}\|\xi(t)\|_\infty \end{aligned}$$

Thus, for every $\underline{\lambda}(A_{22}) > \lambda^*$ we have

$$\begin{aligned} \lim_{t\to\infty} |x_1(t;0,\xi)| &\leq \tfrac{\lambda^*\|B\|}{(\underline{\lambda}(A_{22})-\lambda^*)\|A_{21}\|}\ \|\xi(t)\|_\infty \\ \lim_{t\to\infty} |x_2(t;0,\xi)| &\leq \tfrac{\|B\|}{\underline{\lambda}(A_{22})-\lambda^*}\ \|\xi(t)\|_\infty \end{aligned} \tag{29}$$

Clearly, from (25), (26) and (29), the inequalities (24) are satisfied and for $\underline{\lambda}(A_{22}) \to \infty$, the time response of the interconnected system (23) converges to zero as $t \to \infty$.

References

Adhami-Mirhosseini, A., A.P. Aguiar and M.J. Yazdanpanah (2011). Seabed tracking of an autonomous underwater vehicle with nonlinear output regulation. In 'Proc. 50th IEEE conference on decision and control'. Maui, Hawaii.

Bennett, A., J.J. Leonard and J.G. Bellingham (1995). Bottom following for survey-class autonomous underwater vehicles. In 'Proceedings of the International Symposium on Unmanned Untethered Submersible Technology'. University of New Hampshire-Marine Systems. pp. 327–336.

Caccia, M., R. Bono, G. Bruzzone and G. Veruggio (2003). 'Bottom-following for remotely operated vehicles'. *Control Engineering Practice* **11**, 461–470.

Fornberg, B. (1996). *A Practical Guide to Pseudospectral Methods*. Cambridge university press. Cambridge, UK.

Fossen, T. (1994). *Guidance and Control of Ocean Vehicles*. John Wiley and Sons. New York.

Funaro, D. (1991). *Polynomial Approximation of Differential Equations*. Speringer-Verlag. Berlin, Germany.

Huang, J. (2004). *Nonlinear Output Regulation: Theory and applications*. SIAM. Philadelphia.

Isidori, A. (1995). *Nonlinear Control Systems*. Springer-Verlag. London.

Jalving, B. (1994). 'The ndre-auv flight control system'. *IEEE Journal of Ocean Engineering* **19**(4), 497–501.

Marconi, L. and L. Praly (2008). 'Uniform practical nonlinear output regulation'. *Automatic Control, IEEE Transactions on* **53**, 1184–1202.

Pavlov, A., N. van de Wouw and H. Nijmeijer (2006). *Uniform Output Regulation Of Nonlinear Systems*. Birkhauser. Boston.

Silvestre, C., R. Cunha, N. Paulino and A. Pascoal (2009). 'A bottom-following preview controller for autonomous underwater vehicles'. *IEEE Transaction on Control Systems Technology* **17**, 257–266.

Steffens, K. (2006). *The History of Approximation Theory: From Euler to Bernstein*. Birkhauser. Boston.

Zames, G. (1966). 'On the input-output stability of time-varying nonlinear feedback systems - parts i and ii'. *Automatic Control, IEEE Transactions on* **11**, 228–238, 465–476.